Error Performance Analysis of Clipped Alamouti Space-Time Coded OFDM Systems

Himal A. Suraweera and Jean Armstrong
Department of Electrical and Computer Systems Engineering
Monash University
Melbourne Victoria 3800, Australia
E-mail: {himal.suraweera, jean.armstrong}@eng.monash.edu.au

***Abstract*— In this paper we investigate the performance of clipped Alamouti space-time coded (STC) orthogonal frequency division multiplexing (OFDM) systems. The high peaks in STC-OFDM signals are clipped to limit the peak-to-average power ratio (PAPR). In STC-OFDM and OFDM, clipping can achieve significant PAPR reduction while maintaining a low symbol error rate (SER). Previous studies on OFDM have concluded that the effect of channel fading on clipping noise must be considered for an accurate error performance analysis. We extend this further to incorporate STC-OFDM systems and jointly study the impact of channel fading and receiver combining on clipping noise. At the STC-OFDM receiver, effective clipping noise governing the signal-to-noise ratio has different characteristics compared to the same for OFDM. Simulations indicate that STC-OFDM is more sensitive to clipping effects than OFDM. The theoretical and simulated SER are also compared for clipped STC-OFDM.**

I. Introduction

Multiple-input multiple-output (MIMO) systems in combination with orthogonal frequency division multiplexing (OFDM) technology is an attractive way of realizing the high data rates required for future communication links. OFDM is effective in mitigating the frequency selectivity encountered in typical fading scenarios and MIMO techniques are capable of providing transmission reliability over wireless channels. OFDM systems with transmit and/or receive diversity can be implemented using either spatial multiplexing, space time-frequency coding or delay diversity techniques [1]-[3]. MIMO-OFDM technology is currently in the process of been standardized for the high speed IEEE WLAN 802.11.n standard.

However a drawback of OFDM is the high peak-to-average power ratio (PAPR) [4]-[8]. The real and imaginary components of the time domain OFDM signals are approximately Gaussian distributed and exhibit sporadic high peaks. Since the MIMO-OFDM transmitter is essentially based on OFDM, large amplitude signals arise in MIMO-OFDM transmissions as well [4], [6]. High PAPR can cause the transmitter power amplifier to saturate introducing spectral spreading and non-linear distortion. As a result OFDM transmitters require highly linear power amplifiers with large dynamic range which are inefficient, expensive and can cause excessive drain on the portable equipment.

Previous published works on PAPR have presented a number of techniques to reduce the high signal peaks. These include techniques designed for OFDM and MIMO-OFDM. Many of the proposed PAPR reduction schemes for OFDM need to be substantially modified to be able to apply for MIMO-OFDM. Hence clipping seems to be the most simple and attractive solution requiring less computational effort at the transmitter and the receiver [4], [7]. Especially for MIMO-OFDM other proposed PAPR reduction techniques can be computationally costly [6].

For OFDM transmission clipping effects have been analyzed extensively over additive white Gaussian noise (AWGN) and frequency selective fading channels [5], [8], [9]. Previously it has been shown using Bussgang's theorem that clipping introduces constellation shrinkage for the OFDM signal [8], [9]. Although effective in reducing high signal peaks, clipping generates both in-band and out-of-band (OOB) distortion. The amount of in-band distortion establishes the error performance of an OFDM system while the OOB distortion must be kept to a minimum to avoid any adjacent channel interference.

In this paper we investigate the performance of an amplitude clipped Alamouti space-time coded OFDM (STC-OFDM) system. To our best knowledge clipping effects for STC-OFDM have not presented in the past literature. Several differences between OFDM and STC-OFDM employing clipping are are worth mentioning. In STC-OFDM two consecutive OFDM symbols transmitted from the two antennas are used to detect the transmitted values on subcarriers. Hence the clipping noise due to the four symbols must be jointly considered for an accurate performance analysis. When the clipping level is high

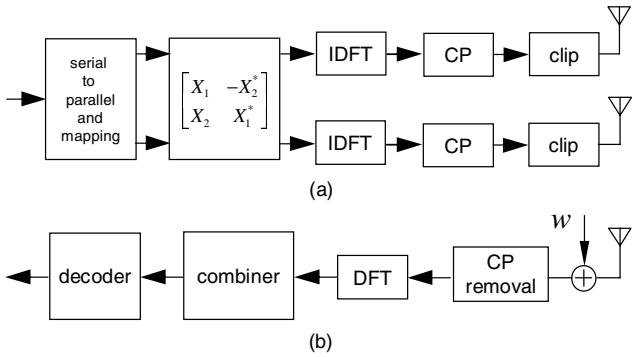

Fig. 1. Block diagram of a clipped Alamouti STC-OFDM system. (a) Transmitter (b) Receiver.

only some transmitted symbols are clipped and this effect must be accounted in the performance analysis. This is because of the statistical nature associated with the occurrence of the high peaks. The maximum-likelihood decoding employed at the STC-OFDM receiver decouples the signals transmitted from the different antennas. Hence the channel faded clipping noise is affected by the coefficients used in combining. This is not the case in OFDM. In the two systems, the effective clipping noise that degrade the signal-to-noise ratio (SNR) for the decision variables exhibits different characteristics. We show that STC-OFDM is more sensitive to clipping effects compared to OFDM. Results for the theoretical error performance are also provided where they are verified from simulations.

The rest of the paper is organized as follows. In Section II we introduce the Alamouti coded OFDM model and study the signal envelope statistics. Next a detailed description of the clipping system is presented. The performance analysis of clipped STC-OFDM is investigated in Section III. Simulation results are presented in Section IV. Finally concluding remarks appear in Section V.

II. Alamouti Coded OFDM Model

Without loss of generality, in what follows we describe an STC-OFDM system based on the Alamouti code using $n_T = 2$ transmit and $n_R = 1$ receive antennas [3]. At the OFDM transmitter incoming data bits are divided and mapped onto a signal alphabet $\mathcal{X}$ before Alamouti mapping. For 4-QAM, $\mathcal{X} \in (\pm 1 \pm j)$. Let us consider the use of OFDM with Alamouti coding [2]. In this case there are two possible coding options. Assuming that the channel remains constant over two consecutive OFDM symbol periods, the OFDM symbols X_1 and X_2 are transmitted from antenna 1 and 2. Then during the next symbol period $-X_2^*$ and X_1^* are transmitted from the same antenna pair. Here X^* denotes the complex conjugate of X. In the following this is referred to as STC-OFDM. The transmitted STC-OFDM symbols are given by

$$\begin{pmatrix} \mathbf{X}_1 \\ \mathbf{X}_2 \end{pmatrix} \rightarrow \begin{pmatrix} \mathbf{X}_1 & -\mathbf{X}_2^* \\ \mathbf{X}_2 & \mathbf{X}_1^* \end{pmatrix} \begin{matrix} \rightarrow \\ \downarrow \end{matrix} \begin{matrix} \text{time} \\ \text{space} \end{matrix} \tag{1}$$

This STC-OFDM system extracts the available spatial diversity of the fading channel on a per subcarrier basis hence experiences a diversity order of 2. However since the OFDM symbol period is usually large the use of STC-OFDM may be an impractical option in fast fading channels. The requirement that the channel remains to be constant over two consecutive OFDM symbol periods may not be satisfied. In the following a quasi-static Rayleigh fading channel is assumed. This is not a limitation, since in our subsequent analysis on STC-OFDM can be applied to Space-frequency coded OFDM systems used in fast fading channels. In SFC-OFDM, the Alamouti coding is performed along the subcarriers. The transmitted SFC-OFDM symbols are given by

$$\begin{aligned} \mathbf{X}_1 &= [X(1), -X^*(1), \cdots, X(N-2), -X^*(N-1)]^T \\ \mathbf{X}_2 &= [X(1), X^*(0), \cdots, X(N-2), X^*(N-1)]^T \end{aligned} \tag{2}$$

A. STC-OFDM Signal Statistics

In this section we study the STC-OFDM signal envelope characteristics. The distribution of the continuous-time domain STC-OFDM signal envelope or PAPR cannot be evaluated accurately by sampling the signal at Nyquist rate. Hence oversampling is essential to produce accurate signal envelope estimates. The discrete time domain OFDM signal oversampled by a factor of J is given by

$$x(n) = \frac{1}{\sqrt{N}} \sum_{k=0}^{N-1} X(k) \exp\left(\frac{j2\pi nk}{JN}\right) \tag{3}$$

for $n = 0, 1, \cdots, (JN-1)$. Oversampling is performed by extending the input frequency domain vector by padding $(J-1)N$ zeros in the middle before taking the IDFT.

More recently it was reported in [10] that to properly estimate the spectral regrowth due to the power amplifier nonlinearity acting on the signal one must consider the signal statistics rather than the PAPR. The reasoning behind this argument was that the amount of distortion generated strictly depends on the dynamic interaction between the signal and the nonlinearity. Although in the following ideal linear characteristics for the power amplifier is assumed after clipping, the same is true for investigating the clipping effects. The signal envelope statistics and PAPR characteristics for STC-OFDM and OFDM are similar. This can be intuitively explained as follows. Assuming independent equally likely points to be transmitted from the two antennas, for STC-OFDM Alamouti mapping will generate complex conjugate symbols. However due to the symmetry of the M-QAM alphabet these will also be valid signal points. More mathematically noting that the following IDFT relationship [11, pp. 568]

$$x^*[((-n))_N] \leftrightarrow X^*[k] \tag{4}$$

We see that the systems must have similar characteristics. Fig. 2 shows the complementary cumulative distribution function

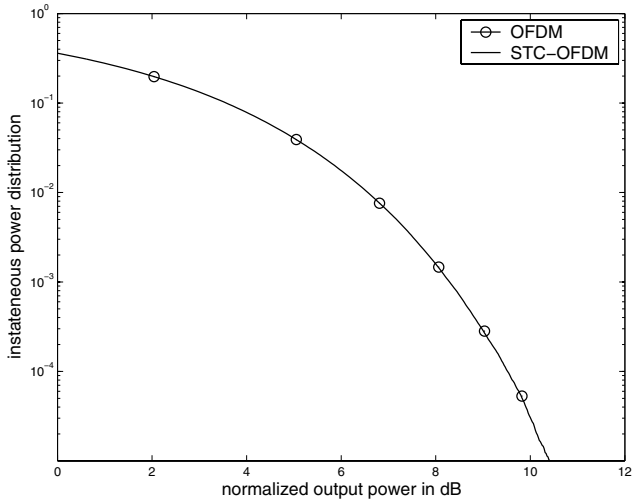

Fig. 2. Complementary cumulative density function of instanteneous power for OFDM and STC-OFDM signals. $N = 64$ and 4-QAM was used.

(CCDF) of the normalized instantaneous power distribution for OFDM and STC-OFDM.

B. Clipped STC-OFDM Signals

The oversampled time domain STC-OFDM signals are clipped to reduce the peak power. This signal is low-pass filtered, upconverted using a carrier frequency f_c before transmission to the channel.

The signals after the IDFT have occasional high peaks. Hence using the following limiter function $x(n)$ is clipped.

$$f\{x(n)\} = \hat{x}(n) = \begin{cases} x(n) & |x(n)| \leq A \\ Ae^{j\arg\{x(n)\}} & |x(n)| \geq A \end{cases} \quad (5)$$

Clipping ratio (CR) is often used as a measure of clipping. CR is defined as the ratio of the maximum clipping amplitude A to the root-mean-square power σ of the unclipped baseband signal [5].

$$\text{CR} = 20\log_{10}\left(\frac{A}{\sigma}\right) \text{ dB}. \quad (6)$$

Since the time domain real and imaginary OFDM signal components are approximately Gaussian distributed, clipping introduced nonlinear distortion can be analyzed using the Bussgang's theorem [8], [9]. This theorem states that a Gaussian signal subjected to a nonlinearity can be expressed as the sum of useful scaled input signal and an uncorrelated nonlinear distortion noise term [8], [9]. Since STC-OFDM and OFDM signals have similar characteristics Bussgang's theorem is also invoked to analyze clipping effects in STC-OFDM. Let $\hat{x}_i(n)$ denote the discrete time transmitted STC-OFDM signal from the ith antenna,

$$\hat{x}_i(n) = \alpha x_i(n) + d_i(n) \quad (7)$$

where α is the shrinkage constant which reflects the power loss due to clipping process and $d(n)$ is the clipping noise. In (7) α is theoretically expressed by [9]

$$\alpha = \frac{1}{\sigma^4}\int_0^\infty f(r)\, r^2 e^{\frac{-r^2}{2\sigma^2}} dr,\ r \geq 0 \quad (8)$$

where $r = |x(n)|$ and in the case of amplitude clipping using (5) α can be further simplified.

$$\alpha = (1 - e^{\frac{-A^2}{\sigma^2}}) + \sqrt{\frac{\pi A^2}{4\sigma^2}}\ \text{erfc}\left(\frac{A}{\sigma}\right) \quad (9)$$

where $\text{erfc}(\cdot) = 2/\sqrt{\pi}\int_x^\infty e^{-y^2}dy$. Fig. 3 shows the graph of attenuation coefficient α against the CR in dB. For comparison simulated results are also presented where they agree exactly with the theoretical expression. The constellation shrinkage is negligible for CR > 8 dB, i.e., $\alpha = 1$.

III. SER Analysis of Clipped STC-OFDM

In this Section we study the theoretical error performance of clipped STC-OFDM. The data carrying subcarriers use M-QAM constellation points. The performance of clipped STC-OFDM signals can be analyzed using some results reported in previous publications on OFDM [9]. However several

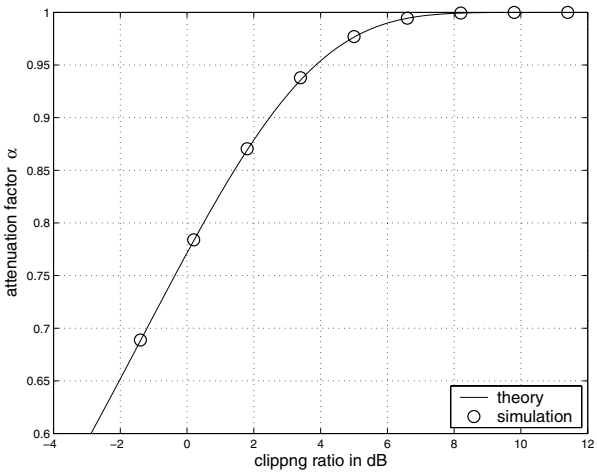

Fig. 3. Attenuation factor α versus clipping ratio.

modifications are required due to the Alamouti mapping and receiver combining.

Denoting $\mathbf{r}(n)$ as the received signal, $\mathbf{r}(n)$ is

$$\mathbf{r}(n) = \sum_{l=0}^{L-1} \mathbf{h}_l \hat{\mathbf{x}}(n-l) + \mathbf{w}(n) \quad (10)$$

The complex $n_R \times n_T$ matrix $\mathbf{h}_l$ represents entries from the lth tap of the channel and $\hat{\mathbf{x}}(n)$ is the $n_T \times 1$ signal vector $[x_1(n), x_2(n)]^T$. $\mathbf{h}_l$ contains circularly symmetric Gaussian variables with zero mean and variance σ_l^2, where σ_l^2 is derived from the channel power delay profile. $w(n)$ is the circularly symmetric AWGN component $w(n) \backsim \mathcal{N}(0, \sigma_w^2)$.

The vector $\mathbf{r}(n)$, $n = 0, ..., (N-1)$ is passed through an N-point DFT to obtain the frequency domain signals. Hence the discrete frequency domain received signals for the kth subcarrier $R_k^{(i)}$ over two consecutive symbols periods, $2i$ and $(2i+1)$ are given by

$$\begin{aligned} R_k^{(2i)} &= \alpha(H_{1,k}X_{1,k} + H_{2,k}X_{2,k}) \\ &\quad + (H_{1,k}D_{1,k}^{(2i)} + H_{2,k}D_{2,k}^{(2i)}) + W_k^{(2i)} \end{aligned} \quad (11)$$

$$\begin{aligned} R_k^{(2i+1)} &= -\alpha(H_{1,k}X_{2,k}^* - H_{2,k}X_{1,k}^*) \\ &\quad + (H_{1,k}D_{1,k}^{(2i+1)} + H_{2,k}D_{2,k}^{(2i+1)}) + W_k^{(2i+1)} \end{aligned} \quad (12)$$

We have omitted the power normalization factor from $(11) - (12)$ for equation brevity. In the linear maximum-likelihood detector, the decision variables $\tilde{X}_1, \tilde{X}_2$ are formulated to estimate the values X_1, X_2 mapped onto the kth STC-OFDM subcarrier using the following combinations [2].

$$\tilde{X}_{1,k} = H_{1,k}^* R_k^{(2i)} + H_{2,k} R_k^{*(2i+1)} \quad (13)$$

$$\tilde{X}_{2,k} = H_{2,k}^* R_k^{(2i)} - H_{1,k} R_k^{*(2i+1)} \quad (14)$$

In (11) and (12) $D_{1,k}, D_{2,k}$ are the frequency domain clipping noise components. Although here we subscript the clipping noise due to the two transmitting antennas separately, the two

processes have identical characteristics. $D_{1,k}$ is written by

$$D_{1,k} = \frac{1}{\sqrt{JN}} \sum_{n=0}^{JN-1} d_1(n) \exp\left(-\frac{j2\pi nk}{JN}\right) \quad (15)$$

A similar expression follows for $D_{2,k}$. For CR values not too high, the frequency domain clipping noise can be accurately modeled by a zero mean complex Gaussian process with power $\sigma^2_{D,k}$ [8], [9], [12]. In the case of Nyquist rate clipping, all the components of clipping noise falls in-band resulting a simple theoretical expression for $\sigma^2_{D,k}$ and for oversampled signals, the approaches in [9], [13] derive the exact power spectral density of $D_{1,k}$ and $D_{2,k}$. These values can be used to establish the post detected SNR for the decision variables $\tilde{X}_1, \tilde{X}_2$ and then to evaluate the theoretical SER.

Consider the decision statistic $\tilde{X}_{1,k}$ for $X_{1,k}$. We expand (13) using $(11) - (12)$ to get

$$\begin{aligned} \tilde{X}_{1,k} &= \alpha(|H_{1,k}|^2 + |H_{2,k}|^2)X_{1,k} \\ &+ |H_{1,k}|^2 D^{(2i)}_{1,k} + |H_{2,k}|^2 D^{(2i+1)}_{2,k} \\ &+ H^*_{1,k} H_{2,k} (D^{*(2i+1)}_{1,k} + D^{(2i)}_{2,k}) \\ &+ H^*_{1,k} W^{(2i)}_k + H_{2,k} W^{(2i+1)}_k \end{aligned} \quad (16)$$

The combination of frequency domain components of the clipping noise and AWGN reduce the effective SNR for the post DFT detected subcarriers. The error performance of OFDM in both AWGN and fading channels has been well studied [5], [9]. In [5] it was reported that in frequency selective fading channels, the performance degradation due to clipping for SISO-OFDM is minimal. Clipping noise is added at the transmitter and fades along with the useful signal. OFDM subcarriers in deep fade which governs the system error performance are least affected by the clipping noise [5]. However in STC-OFDM the channel coefficients used in combining process must be considered to analyze the impact of clipping noise on the SER. The following analysis includes establishing the effective SNR for the decision variables $\tilde{X}_1$ and $\tilde{X}_2$. Next this is used for the SER computation.

In the dual transmit single receive antenna fading channel, the SNR γ_k for $\tilde{X}_1$ is given by

$$\gamma_k = \frac{\alpha^2(|H_{1,k}|^2 + |H_{2,k}|^2)\sigma^2_X}{\lambda\sigma^2_D + 2\sigma^2_W} \quad (17)$$

where σ^2_X is the averaged constellation power and λ is

$$\lambda = \left| \sqrt{|H_{1,k}|^2 + |H_{2,k}|^2} + \frac{2H^*_{1,k}H_{2,k}}{\sqrt{|H_{1,k}|^2 + |H_{2,k}|^2}} \right|^2 \quad (18)$$

The unclipped SNR after combining $\gamma = \frac{(|H_{1,k}|^2 + |H_{2,k}|^2)\sigma^2_X}{n_T\sigma^2_W}$ is a χ^2 distributed random variable with 4 degrees of freedom. $P(\gamma)$ the probability density function (PDF) of γ and can be easily determined by a characteristic function approach [14]. Assuming that the two channel paths are independent, and using the characteristic function $P(\gamma)$ can be expressed as

$$P(\gamma) = \frac{\gamma}{\bar{\gamma}^2} \exp(-\gamma/\bar{\gamma}) \quad (19)$$

In (19) $\bar{\gamma} = \frac{\sigma^2_X}{n_T\sigma^2_W}$. The SER for the kth subcarrier, $P_{E,k}$ as a function of the instantaneous SNR is given by

$$P_{E,k} = \int_0^\infty P_M(\gamma)P(\gamma)d\gamma \quad (20)$$

and for M-QAM $P_M(\gamma)$ is approximately given by [14] (pp. 280)

$$P_M(\gamma) = 2a \times \text{erfc}\left(\sqrt{\frac{\gamma}{b}}\right) - a^2 \times \text{erfc}^2\left(\sqrt{\frac{\gamma}{b}}\right) \quad (21)$$

where $a = 4(1 - 1/\sqrt{M})$, $b = 2(M-1)/(3\log_2 M)$ and the complementary error function $\text{erfc}(x) = 2/\sqrt{\pi}\int_x^\infty e^{-t^2}dt$. Hence for a 16-QAM clipped STC-OFDM system, the theoretical SER can be approximately calculated as

$$\begin{aligned} P_{E,k} \approx \frac{2a}{\bar{\gamma}^2} \int_0^\infty \gamma \, \text{erfc}\left(\sqrt{\frac{\alpha^2\gamma}{b(\gamma\sigma^2_D + 1)}}\right) \\ \times \left(1 - \frac{a}{2}\text{erfc}\left(\sqrt{\frac{\alpha^2\gamma}{b(\gamma\sigma^2_D + 1)}}\right)\right) \exp\left(-\frac{\gamma}{\bar{\gamma}}\right) \, d\gamma \end{aligned} \quad (22)$$

Note that we have simplified the effective clipping noise contribution for the instantaneous SNR when expressing (22). A more accurate theoretical SER must consider the exact PDF of λ but this approach is more complex and probably involves a double integration. In this paper we have used Monte-Carlo integration to calculate the integral form theoretical expression in (22). The approximated results indicate a good degree of accuracy compared with the simulations. Finally the total averaged SER can be obtained as the mean of $P_{E,k}$. When oversampling is employed, clipping noise characteristics slightly deviate per subcarrier basis and is not exactly white. Hence even in a flat Rayleigh fading channel, one would need to initially evaluate the individual SER for each subcarrier before calculating the total averaged SER. From a practical point of view and for lower order modulation schemes including BPSK, QPSK and 4-QAM this may not have a significant impact. This work is beyond the scope of the paper.

A. Case: SER at Low SNR

At low SNR and at high CR, the AWGN compared to clipping noise is significant and establish the achievable performance. The SER $P^{(\text{LSNR})}_{E,k}$ can be approximately evaluated or lower bounded using a standard STC-OFDM receiver. In this case we can calculate $P^{(\text{LSNR})}_{E,k}$ in closed form.

$$\begin{aligned} P^{(\text{LSNR})}_{E,k} \approx \frac{2a}{\bar{\gamma}^2} \int_0^\infty \gamma \, \text{erfc}\left(\sqrt{\frac{\alpha^2\gamma}{b}}\right) \\ \times \left(1 - \frac{a}{2}\text{erfc}\left(\sqrt{\frac{\alpha^2\gamma}{b}}\right)\right) \exp\left(-\frac{\gamma}{\bar{\gamma}}\right) \, d\gamma \end{aligned} \quad (23)$$

The first integral I_1 in (23) can be solved using integration by parts and an integral result of [15, (2.8.5-6)].

$$I_1 = \frac{2a}{\bar{\gamma}^2}\int_0^\infty \gamma \,\mathrm{erfc}\left(\sqrt{\frac{\gamma}{b}}\right)\exp\left(-\frac{\gamma}{\bar{\gamma}}\right)\,d\gamma \qquad (24)$$
$$= 2a - 3a\sqrt{\frac{\bar{\gamma}}{b}}\,{}_2F_1\left(\frac{1}{2},\frac{5}{2};\frac{3}{2};-\frac{\bar{\gamma}}{b}\right)$$

where ${}_2F_1(x_1, x_2; x_3; x_4)$ is the Gauss hypergeometric function defined by

$${}_2F_1(x_1, x_2; x_3; x_4) = \sum_{n=0}^{\infty}\frac{(x_1)_n(x_2)_n}{(x_3)_n n!}x_4^n \qquad (25)$$

and $(x)_n = x(x+1)...(x+n-1)$ is the Pochhammer symbol. Similarly the second integral I_2 can be evaluated by

$$I_2 = \frac{a^2}{\bar{\gamma}^2}\int_0^\infty \gamma \,\mathrm{erfc}^2\left(\sqrt{\frac{\gamma}{b}}\right)\exp\left(-\frac{\gamma}{\bar{\gamma}}\right)\,d\gamma \qquad (26)$$
$$= -\frac{\bar{\gamma}\beta^{3/2}}{2b} + \frac{2\bar{\gamma}\beta^2}{\pi b}\,{}_2F_1\left(\frac{1}{2},2;\frac{3}{2};-\beta\right)$$
$$-\frac{\bar{\gamma}^2\beta^{1/2}}{b^2} + \frac{2\bar{\gamma}^2\beta}{\pi b^2}\,{}_2F_1\left(\frac{1}{2},1;\frac{3}{2};-\beta\right)$$

where $\beta = 1/(1+\frac{b}{\bar{\gamma}})$ and we get $P_{E,k}^{(\mathrm{LSNR})} = I_1 + I_2$.

B. Case: SER at High SNR

At high SNR the AWGN component is negligible and the system degradation is mainly due to the clipping noise added at the transmitter. In this case SER is approximately equal to the AWGN receiver performance, i.e., AWGN power to be replaced by the clipping noise power. This is not surprising as both the OFDM signal and the clipping noise are faded together and the fading effect on them is cancelled. Hence SER is directly given by (21) and $\gamma = \frac{\alpha^2\sigma_X^2}{\sigma_{D,k}^2}$.

IV. Simulation Results

In this Section the simulated and theoretical error performance results for clipped STC-OFDM are reported. For simulated results we have used $J = 4$ which is sufficient to detect the true signal peaks [7]. Perfect channel state information and synchronization was assumed at the receiver. Channel power delay profile was assumed to be uniformly distributed with $L = 3$. For the simulations $N = 64$ and 16-QAM modulation was used. $E\{ww^*\} = N_0$.

Fig. 4 shows the SER performance of a clipped 16-QAM STC-OFDM system. When CR $>$ 7 dB the clipped system almost shows a similar performance compared to an unclipped STC-OFDM system, marginally suffering some degradation. However when the clipping level is further reduced (for CR $<$ 6.5 dB) the SER curves exhibit an error floor after $E_b/N_0 = 30$ dB and for CR $<$ 4.5 dB the error floor occurs approximately after $E_b/N_0 = 25$ dB. Clipping noise influence on the error performance is substantial at low CR. Previous studies on OFDM have concluded that the effect of channel fading on clipping noise must be considered for an accurate error performance analysis [5]. Although the clipping noise

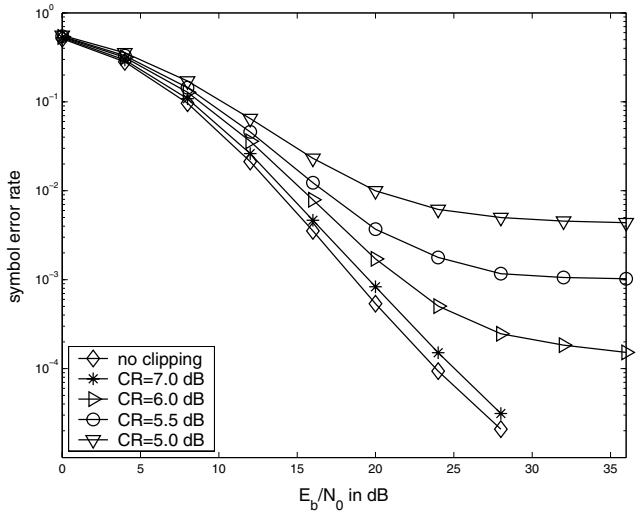

Fig. 4. SER against E_b/N_0 of clipped STC-OFDM.

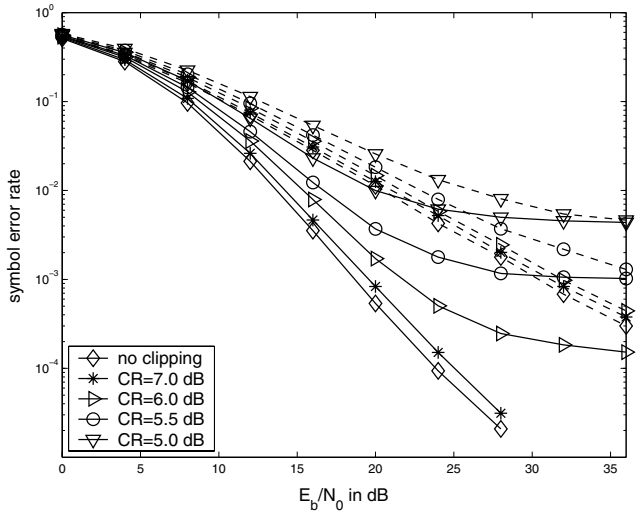

Fig. 5. SER performance comparison of clipped OFDM and STC-OFDM. The dash-line plots are for OFDM.

fades in the dual transmit frequency selective channel, the effective clipping noise establishing the SNR for the post DFT detected decision variables after linear maximum-likelihood combining at the receiver, seems to be more robust than the same in an SISO Rayleigh fading scenario.

This is further explained from the results of Fig. 5 where an SER comparison is shown for OFDM and STC-OFDM. The dashed lines represent the results for OFDM. As expected in the simulated E_b/N_0 range even clipped STC-OFDM for CR $>$ 6 dB shows a better performance than a conventional OFDM. This is due to the diversity advantage of the STC-OFDM system. However plots in Fig. 5 also indicate that STC-OFDM is more sensitive to clipping effects than SISO-OFDM. Let us consider the cases of "no clipping" and "clipped CR $=$ 6 dB". The STC-OFDM system exhibits both a considerable deviation from the ideal performance and an error floor. For the same CR, OFDM system also shows some degradation but

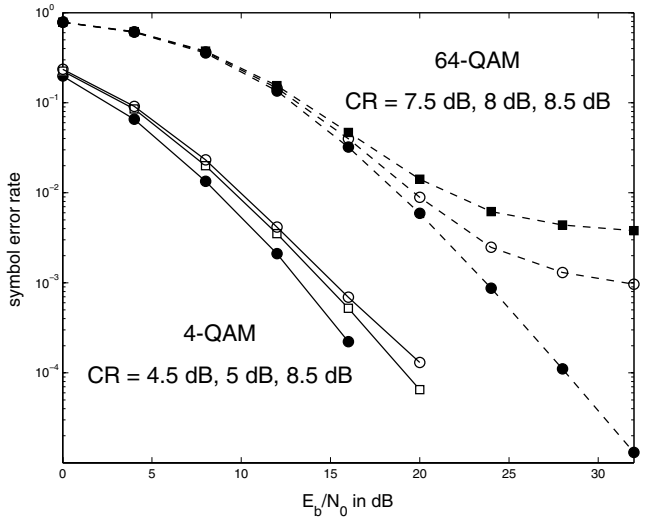

Fig. 6. SER performance of 4 and 64-QAM clipped STC-OFDM.

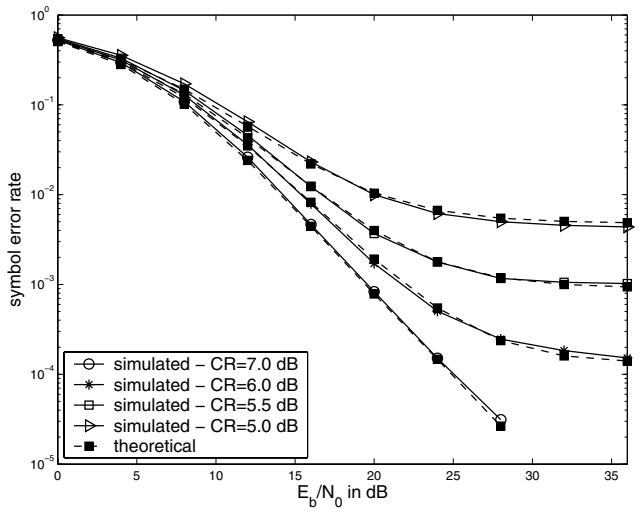

Fig. 7. Semi-theoretical and simulated SER performance comparison of clipped STC-OFDM using 16-QAM.

the deviation from the ideal "no clipping" case is small. This trend is also noticeable for higher levels of clipping.

Fig. 6 shows the SER against E_b/N_0 for STC-OFDM using different CR and modulation schemes of 4-QAM and 64-QAM. At high E_b/N_0 the 64-QAM plots indicate an observable plateau for CR $= 7.5$ and 8 dB. The error degradation due to clipping for 4-QAM is negligible even at CR $= 5$ dB. Fig. 7 shows the results of a theoretical and simulated SER comparison for an 16-QAM clipped STC-OFDM system. In rapid system prototyping the theoretical results are helpful in determining the tolerable clipping levels to guarantee a pre defined receiver error performance. Simulations were used to calculate an average clipping noise power considering all subcarriers when plotting the theoretical curves. For a more accurate result the clipping noise power must be evaluated individually for all subcarriers however as seen from Fig. 7 the simulations closely agree with the predicted results from theory.

V. Conclusions

In this paper we investigated the signal envelope statistics and amplitude clipping effects for an Alamouti STC-OFDM dual transmit and single receive antenna system. Signal envelope distribution of STC-OFDM and OFDM have similar characteristics. In STC-OFDM and OFDM, clipping can achieve significant PAPR reduction while maintaining a low SER. PAPR reduction is obtained without any redundancy and no side information is required at the receiver.

The error performance of clipped STC-OFDM was analyzed considering jointly the effects of channel fading and receiver combining. Simulations show that STC-OFDM is more sensitive to clipping errors than OFDM at very low CR. However as expected clipped STC-OFDM systems for CR > 6 dB, are capable of delivering better SER performance than unclipped OFDM systems. The SER sensitivity of the two systems to clipping errors is different partially due to the clipping noise influence of the post DFT detected decision variables. The theoretical SER analysis was validated with the simulations where they agree closely.

References

[1] A. F. Molisch, M. Z. Win and J. H. Winters, "Space-time-frequency (STF) coding for MIMO-OFDM systems," *IEEE Commun. Lett.*, vol. 6, pp. 370-372, Sept. 2002.

[2] B. Vucetic and J. Yuan, *Space-Time Coding*. Chichester, UK: Wiley, 2003.

[3] Y. Gong and K. B. Letaief, "An efficient space-frequency coded OFDM system for broadband wireless communications," *IEEE Trans. Commun.*, vol. 51, pp. 2019-2029, Nov. 2003.

[4] S. H. Han and J. H. Lee, "An overview of peak-to-average power ratio reduction techniques for multicarrier transmission," *IEEE Wireless Commun.*, vol. 12, pp. 56-65, Apr. 2005.

[5] K. R. Panta and J. Armstrong, "Effects of clipping on the error performance of OFDM in frequency selective fading channels," *IEEE Trans. Wireless Commun.*, vol. 3, pp. 668-671, Mar. 2004.

[6] Y.-L. Lee, Y.-H. You, W.-G. Geon, J.-H. Paik and H.-K. Song, "Peak-to-average power ratio in MIMO-OFDM systems using selective mapping," *IEEE Commun. Lett.*, vol. 7, pp. 575-577, Dec. 2003.

[7] A. D. S. Jayalath and C. Tellambura, "Peak-to-average power ratio of IEEE 802.11.a transmit signals," in *Proc. 6th Int. Symp. Digital Signal Processing for Communication Systems - DSPCS'02*, Sydney, Australia, Jan. 2002, pp. 31-36.

[8] D. Dardari, V. Tralli and A. Vaccari, "A theoretical characterization of nonlinear distortion effects in OFDM systems," *IEEE Trans. Commun.*, vol. 48, pp. 1755-1764, Oct. 2000.

[9] P. Banneli and S. Cacopardi, "Theoretical analysis and performance of OFDM signals in nonlinear AWGN channels," *IEEE Trans. Commun.*, vol. 48, pp. 430-441, Mar. 2000.

[10] J. F. Sevic and M. B. Steer, "On the significance of envelope peak-to-average ratio for estimating the spectral regrowth of an RF/Microwave power amplifier," *IEEE Trans. Microwave Theory Tech.*, vol. 48, pp. 1068-1071, June 2000.

[11] A. V. Oppenheim, R. W. Schafer and J. R. Buck, *Discrete-Time Signal Processing*. 2nd Ed., Singapore, Pearson: 2002.

[12] J. Tellado, L. M. C. Hoo and J. M. Cioffi, "Maximum-likelihood detection of nonlinearly distorted multicarrier symbols by iterative decoding," *IEEE Trans. Commun.*, vol. 51, pp. 218-228, Feb. 2003.

[13] E. Costa, M. Midrio and S. Pupolin, "Impact of amplifier nonlinearities on OFDM transmission system performance," *IEEE Commun. Lett.*, vol. 3, pp. 37-39, Feb. 1999.

[14] J. G. Proakis, *Digital Communications*. 3rd ed., New York: McGraw-Hill, 1995.

[15] A. P. Prudnikov, Y. A. Brychkov and O. I. Marichev, *Integrals and Series*, vol. 2, Gordon and Breach Science Publishers, 1986.